Supplementary Information

The siderophore yersiniabactin binds copper to protect pathogens during infection

Kaveri S. Chaturvedi[1,2,3], Chia S. Hung[1,2,3], Jan R. Crowley[3], Ann E. Stapleton[4], Jeffrey P. Henderson[1,2,3]*

[1]Center for Women's Infectious Diseases Research, [2]Division of Infectious Diseases, [3]Department of Internal Medicine, Washington University School of Medicine, St. Louis, Missouri, United States of America

[4]Department of Medicine, Division of Allergy and Infectious Diseases, University of Washington, Seattle, Washington, United States of America

* Corresponding author:

Center for Women's Infectious Disease Research

Box 8051 Washington University School of Medicine,

660 S. Euclid Ave., St. Louis, MO 63110

Phone: +13143627250

Fax: +13143623203

E-mail: jhenderson@DOM.wustl.edu

This file includes

- Supplementary Methods
- Supplementary Results

Supplementary Methods

Deletion strain construction

UTI89 mutant strains used in this study are listed in Supplementary Table 1. In-frame deletions in UTI89 were made using the red recombinase method, as previously described, using pKD4 or pKD13 as a template[1,2]. To confirm the appropriate deletions, we performed PCR with flanking primers. Antibiotic resistance insertions were removed by transforming the mutant strains with pCP20 expressing the FLP recombinase.

^{13}C and deuterated internal standard preparation

d_4-ferric-yersiniabactin was produced by chemically complementing the salicylate synthase-deficient mutant UTI89Δ*ybtS* during growth in M63 minimal medium supplemented with 50 μM d_6-salicylate and 0.2% unlabeled glycerol. The isotope-labeled supernatant was harvested by centrifugation and confirmed by LC-MS detection of d_4-ferric-yersiniabactin at *m/z* 539 (Supplementary Figure 1). The *m/z* 539 MS/MS product ion spectrum of this ion retained the 187 amu neutral loss as expected for deuterium incorporation in the yersiniabactin phenyl ring.$^{13}C_{21}$- yersiniabactin was produced by growing the siderophore overproducer UTI89Δ*fur* as previously described[3]. The isotope labeled supernatant was harvested by centrifugation and confirmed by LC-MS detection of $^{13}C_{21}$-ferric yersiniabactin at *m/z* 564 (Supplementary Figure 3). $^{13}C_{21}$-ferric yersiniabactin and $^{13}C_{21}$-cupric yersiniabactin were prepared by treating equal volumes of the labeled supernatant with 5 mM ferric chloride or 5 mM copper sulfate, respectively. Solutions were centrifuged in 15 mL falcon tubes at 6,000 rpm for 10 minutes. The supernatant from these metal treated samples was then subjected to preparative chromatography and eluted with 100% methanol.

Yersiniabactin purification

Apo-yersiniabactin was purified from UTI89Δ*entB* culture supernatants, which lack enterobactin or salmochelin. Metal complexes of yersiniabactin were generated by adding 1.0 M ferric chloride or copper sulfate to UTI89Δ*entB* cell culture supernatants to a final concentration of 5 mM. Metal-treated supernatants were incubated for 15 minutes at room temperature and centrifuged for 2 minutes at 14,000 rpm. The supernatant was then applied to a conditioned preparative reverse phase column (Waters Sep-Pak C18 cartridges), washed with 2 mL of 20% methanol and eluted with 1 mL of 80% methanol. A centrifugal evaporator was used to concentrate the eluate. Samples were resuspended in 20% methanol and further purified by high-performance liquid chromatography. Samples were applied to a Resource^{TM} 1 mL RPC column (GE Healthcare). The gradient used was as follows: Solvent A (100% deionized water) was held constant at 98% and solvent B (100% methanol) was held constant at 2% for 2 minutes, followed by a linear gradient where solvent B was increased to 100% over 20 minutes and then held constant at 100% for 2 minutes. Eluted samples were subsequently concentrated in a centrifugal evaporator and resuspended in 100 μL deionized water. Following mass spectrometric confirmation, *apo*-yersiniabactin concentration was determined spectrophotometrically following conversion to ferric-yersiniabactin (ε_{385}=2,884 M^{-1} cm^{-1}) with 5 mM ferric chloride[4].

Statistical analyses

Statistics and graphs were generated using GraphPad Prism 4 (GraphPad Software, La Jolla, CA). For groupwise comparisons of siderophore production, the Mann-Whitney U Test was performed. The *t*-test was used to compare urinary versus rectal strain growth as well as growth differences between paired strains. Analyses of paired strain differences in siderophore production were performed using the Wilcoxon signed rank test for significance.

Supplementary References

1 Datsenko, K. A. & Wanner, B. L. One-step inactivation of chromosomal genes in Escherichia coli K-12 using PCR products. *Proc Natl Acad Sci U S A* 97, 6640-6645, doi:10.1073/pnas.120163297 (2000).

2 Murphy, K. C. & Campellone, K. G. Lambda Red-mediated recombinogenic engineering of enterohemorrhagic and enteropathogenic E. coli. *BMC Mol Biol* 4, 11, doi:10.1186/1471-2199-4-11 (2003).

3 Henderson, J. P. *et al*. Quantitative metabolomics reveals an epigenetic blueprint for iron acquisition in uropathogenic Escherichia coli. *PLoS Pathog* 5, e1000305, doi:10.1371/journal.ppat.1000305 (2009).

4 Haag, H. *et al*. Purification of yersiniabactin: a siderophore and possible virulence factor of Yersinia enterocolitica. *J Gen Microbiol* 139, 2159-2165 (1993).

Supplementary Results

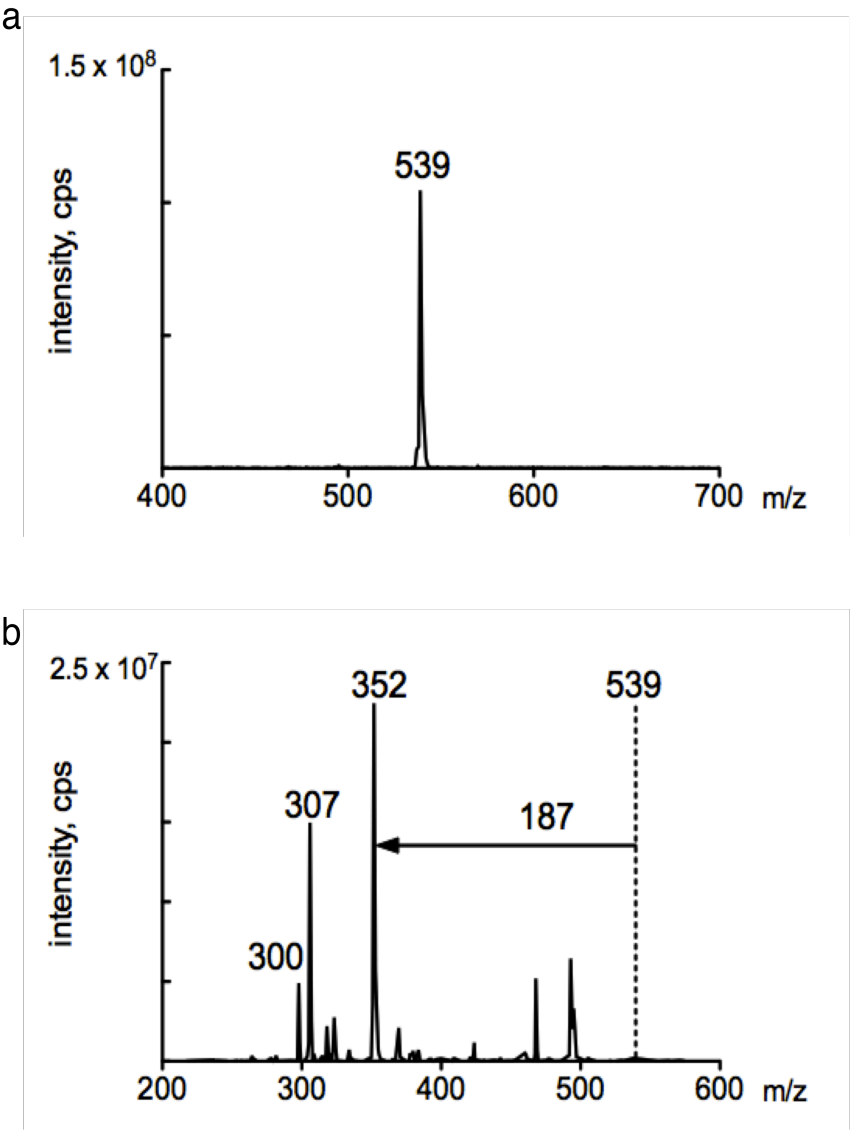

Supplementary Figure 1: Preparation of deuterated yersiniabactin. d_4-ferric-yersiniabactin was produced by chemically complementing the salicylate synthase-deficient mutant UTI89Δ*ybtS* with 50 μM d_6-salicylate during growth in M63 minimal medium containing 0.2% unlabeled glycerol. (a) Full scan positive ion ESI spectrum at the Fe(III)-Ybt retention time reveals an $[M+H]^+$ peak at *m/z* 539, consistent with introduction of the four nonexchangable deuterons in d_6-salicylate. (b) MS/MS of the *m/z* 539 ion revealed a dominant 187 *m/z* unit neutral loss, consistent with neutral loss of a fragment from yersiniabactin's unlabeled carboxylic acid terminus.

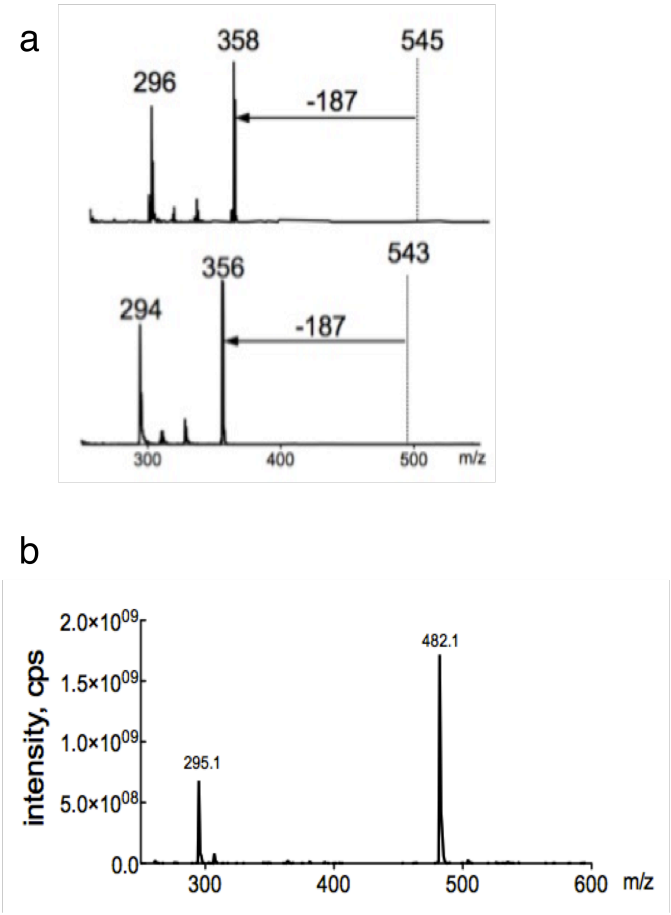

Supplementary Figure 2. Peak 1 is a stable cupric-yersiniabactin complex. (a) MS/MS analysis of the *m/z* 543 and 545 ions from peak 1 confirms the 187 amu neutral loss and shows comparable fragmentation patterns, consistent with natural ^{63}Cu and ^{65}Cu isotope abundances. Addition of cupric sulfate to yersiniabactin-containing culture supernatant generated a robust new peak 1 signal, which was collected for analysis. (b) Mass spectrum of *apo*-yersiniabactin. Depicted is the positive ESI mass spectrum of a sample from the *apo*-yersiniabactin preparation used in this study. The predicted $[M+H]^+$ molecular ion at 482 *m/z* units is evident, along with the $[M+H-187]^+$ source decay fragment at *m/z* 295.

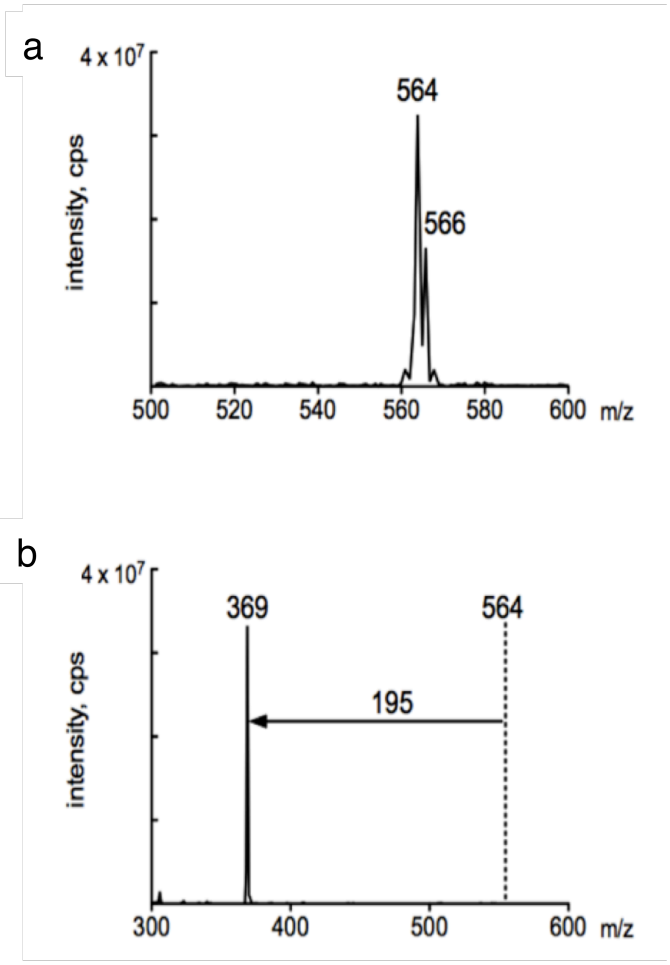

Supplementary Figure 3: Structural confirmation of copper (II)-yersiniabactin complexes by isotope labeling. ^{13}C-labeled internal standard was treated with 3.0 mM copper (II) sulfate and purified over a preparative C18 column. (a) Full scan positive ion ESI spectrum at the Cu(II)-Ybt retention time reveals an $[M+H]^+$ peak at *m/z* 564 and M+2 at *m/z* 566, consistent with ^{13}C-substitution of all 21 carbon atoms in yersiniabactin and the copper M+2 isotope. (b) MS/MS of the *m/z* 564 ion revealed a shifted dominant MS/MS neutral loss of 195 mass units, corresponding to loss of a fragment containing eight carbons.

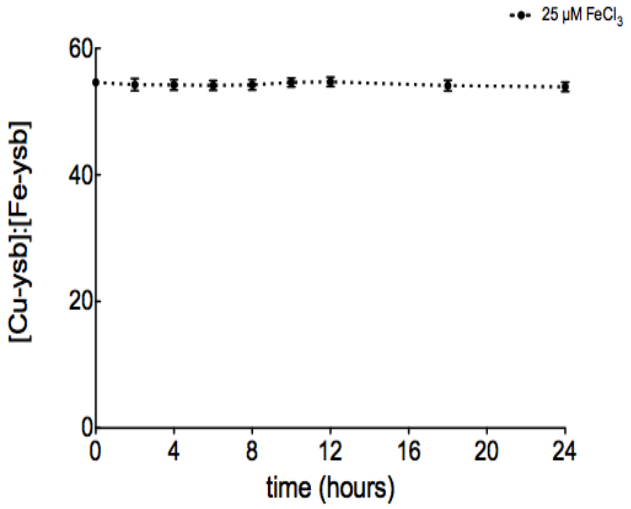

Supplementary Figure 4. The Cu(II)-Ybt complex is stable in the presence of iron. Cu(II)-Ybt complexes are stable and bound copper is not displaced by ferric ions over a period of 24 hours. Cu(II)-Ybt is expressed as its ratio to trace Fe(III)-Ybt impurity in *apo*-Ybt.

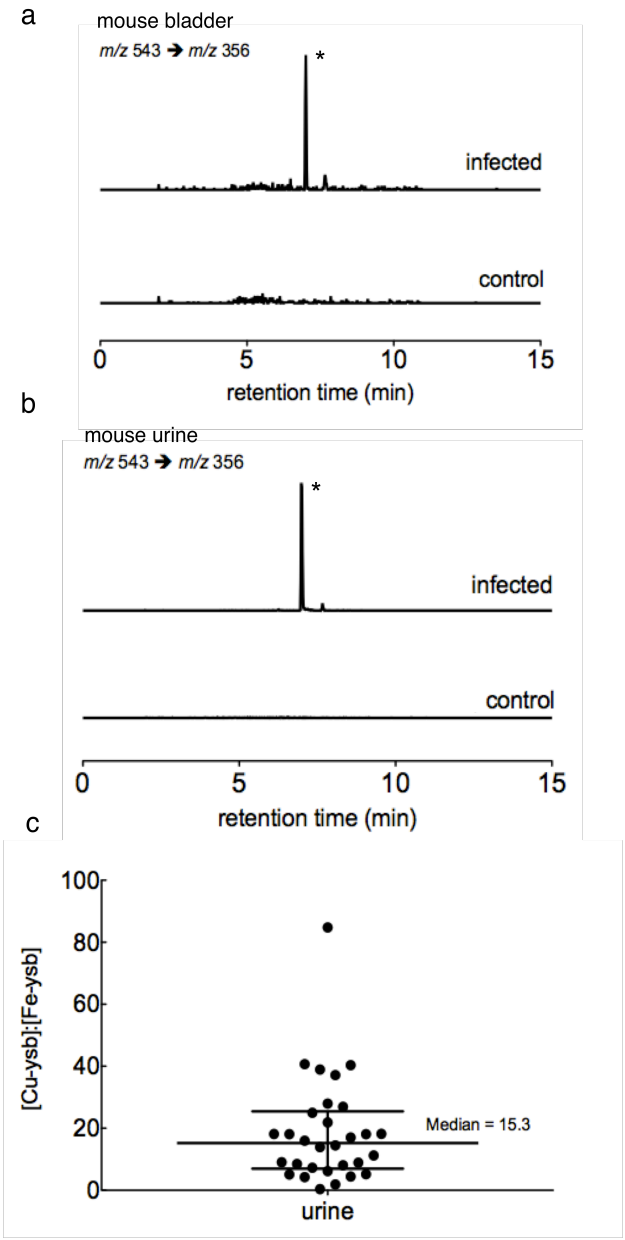

Supplementary Figure 5. Cupric-yersiniabactin forms in murine bladder tissue and urine during experimental uropathogenic *E. coli* cystitis. Bladder tissue and urine were collected from infected mice and prepared for mass spectrometric analysis. Shown are MS/MS chromatograms showing Cu(II)-Ybt peaks in (a) bladder and (b) urine extracts from infected, but not uninfected, animals. (c) In the infected urine samples, the median Cu(II)-Ybt:Fe(III)-Ybt ratio is 15.3, indicating that yersiniabactin preferentially binds copper (II) *in vivo*.

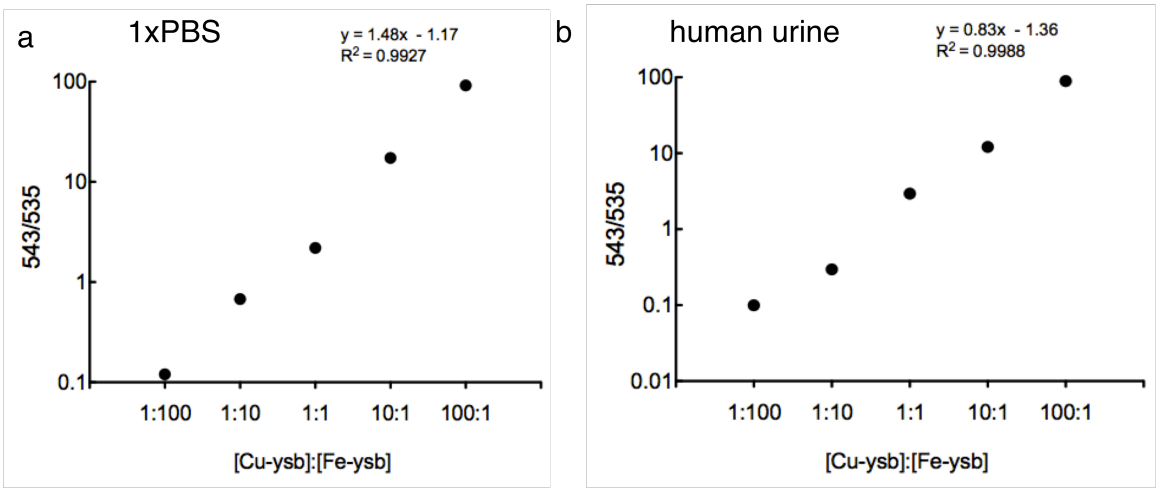

Supplementary Figure 6. Calibration curves for the determination of Cu(II)-Ybt to Fe(III)-Ybt molar ratios. Standard curves used for *in vitro* analysis were performed in phosphate buffered saline (PBS, panel A). Curves used for *in vivo* analyses were performed in human urine (panel B). The Y axes refer to the LC-MS/MS peak area ratios derived from the Cu(II)-Ybt precursor ion at 543 *m/z* units and the Fe(III)-Ybt precursor ion at 535 *m/z* units. Both curves exhibited broad linear responses and slopes near unity.

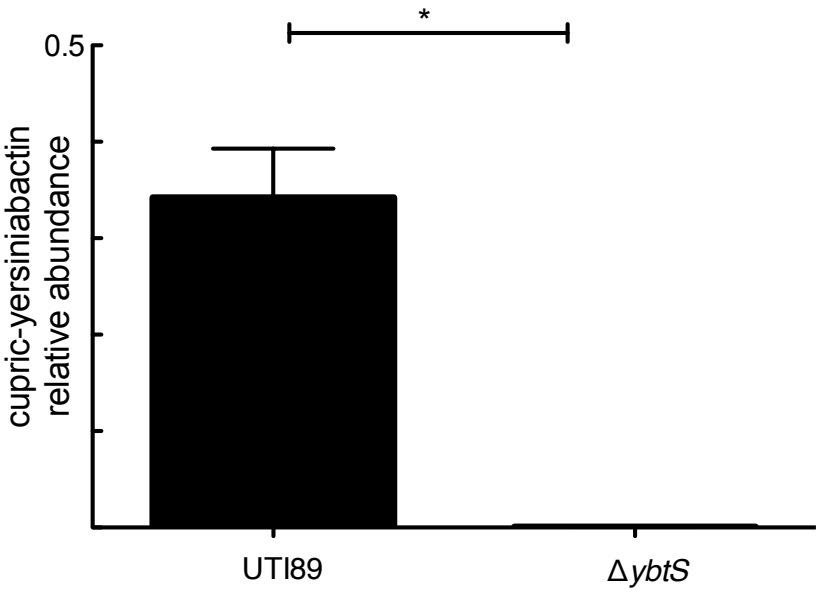

Supplementary Figure 7. LC-MS analysis of wild-type UTI89 and Δ*ybtS* culture supernatants treated with 25 μM copper (II) sulfate. Cu(II)-Ybt complexes were observed in wild type, but not UTI89Δ*ybtS*, conditioned media.

Supplementary Table 1: UTI89 mutant strains used in this study

strain	gene function	reference
UTI89Δ*ybtS*	salicylate synthase, yersiniabactin biosynthesis	3
UTI89Δ*entB*	isochorismate lyase, catecholate siderophore (enterobactin/salmochelin) biosynthesis	3
UTI89Δ*iroA*	salmochelin biosynthesis, transport, catabolism	3
UTI89Δ*entB*Δ*ybtS*	salicylate synthase, isochorismate lyase, total mutant for yersiniabactin, enterobactin and salmochelin biosynthesis	3